

Loss of Heterozygosity Analysis at selected Single Nucleotide Polymorphism Sites in the Intronic Regions of *PAX7* via *In Silico* Biology & Microsatellite Analysis.

*Maika G. Mitchell^{1,2}, Diane Tabarini² Melanie Ziman¹

¹ Faculty of Computing, Health & Science, Edith Cowan University, Perth, W. Australia

² Memorial Sloan Kettering Cancer Center, New York City, New York

Abstract

Motivation. In this study, the eight intronic regions of *PAX7* were scanned for Single Nucleotide Polymorphisms (SNPs), loss of heterozygosity via allele quantification, and tandem repeats that exist immediately before or after the genetic variations.

Method. Culmination of results based on the output of gel electrophoresis and Microsatellite analysis.

Results. The use of less invasive methods, *In Silico* Biology & Microsatellite analysis to identify Rhabdomyosarcoma offering reduced discomfort to cancer patients.

Conclusions. Results of microsatellite analysis show a new method for detecting ERMS/ARMS in patients

Keywords. Single Nucleotide Polymorphisms; *PAX7*; Rhabdomyosarcoma; Loss of heterozygosity; ERMS, ARMS.

Abbreviations and notations

MSI, Microsatellite Instability	chr., chromosome
ARMS, alveolar rhabdomyosarcoma	5', five prime end of DNA strand
3', three prime end of DNA strand	electropherogram, picture file
ERMS, embryonal rhabdomyosarcoma	RD, Rhabdomyosarcoma
CNP, Copy Number Polymorphism	SNP, Single Nucleotide Polymorphism
AQ, Allele Quantification	TSS, transcription start site
LOH, Loss of heterozygosity	SSLP, Simple sequence length polymorphisms
bp, base pair	nt, nucleotide

INTRODUCTION

Testing for the loss of heterozygosity and mutation detection is performed routinely at hospitals across the United States for confirmation of a cancer diagnosis and identification of the molecular lesion [Maris et al., 2005; Kelloff et al., 2006]. Researchers and clinicians have bridged the gap between the discovery and experimentation of new methods to diagnose patients sooner at a molecular level enabling them to create/modify new therapeutics. Much research has been performed on Rhabdomyosarcomas and the chimeric translocation between *PAX7* on chromosome 1 and the Forkhead gene on chromosome 13. In studies performed recently [Hirsch et al., 2001], alveolar rhabdomyosarcoma (ARMS) and embryonal rhabdomyosarcoma (ERMS) have been used to test for single nucleotide polymorphisms (SNPs) which may lead to the location of acquired homozygosity. Thus far, researchers have looked towards chimeric translocations of *PAX7* with other chromosomes (chr.3 & chr.11), (Davis and Barr 1997; Steenman et al., 2000) besides the well known translocation with chromosome 13 (Gattenlöhner et al., 1998). Loss of heterozygosity (LOH) at multiple chromosomal loci is strongly associated with clinical phenotype including patient outcome [Loh et al., 2002].

In this study, the eight intronic regions of *PAX7* were scanned for SNPs that exhibit loss of heterozygosity and were quantified by allele quantification, and tandem/microsatellite repeats that exist immediately before or after the genetic variations. Based on the genotype data stored in the NCBI databank and in house genomic DNA controls, a mutation was detected in one of the seven (14.28%) of the samples tested.

MATERIALS AND METHODS

Tumor Samples & Control Samples

Five ARMS samples were analyzed; all five have *PAX7*-*FKHR* translocations and were obtained from The five ARMS samples were delivered as isolated DNA cores in paraffin, from Biomaxx, Inc. (<http://www.biomax.us/>). All five samples were excised from patient tumour samples. ERMS samples from established cell line ATCC#: CCL 136 and five normal DNA samples isolated from buccal swabs submitted by volunteers were also examined.

LOH Analysis. Primary normal/tumor pairs were investigated using fluorescently labeled microsatellites. Primer sequences were obtained from the Primer3 Database (http://frodo.wi.mit.edu/cgi-bin/primer3/primer3_www.cgi). Amplifications of each microsatellite were done in 7.5- μ l volumes with 10 ng of each respective genomic DNA, 8 pmol of each primer (5' primer, fluorescently labeled), 100 μ M each dNTP, 0.6 unit of AmpliTaq Gold DNA Polymerase (Applied Biosystems, Foster City, CA), 10 mM Tris-HCl (pH 8.3), 50 mM KCl, and 2 mM MgCl₂.

DNA Isolation

EPICENTRE[®] Biotechnologies (<http://www.epibio.com>) BuccalAmp[™] DNA Extraction Kit, QuickExtract[™] DNA Extraction Solution, and Catch-All[™] Sample Collection Swabs were used for the DNA Isolation of the five normal samples submitted by volunteers. The QuickExtract[™] DNA Extraction Solution was also used for the ERMS sample from the cell line ATCC#: CCL 136. The five ARMS samples were delivered as isolated DNA cores formalin fixed, paraffin embedded histology tissue sections. The tissues were fixed by formalin no longer than 48 hours, and then processed to be ready for sectioning. Two serial tissue sections with 5 μ m thickness are mounted on a SuperFrost Plus glass slides.

In Silico Investigation

The introns of *PAX7* were scrutinized with four (3 online, 1 offline) unique programs which store databases of SNPs submitted to the Human Genome Project. The names of the four programs are:

- 1) dbSNP (<http://www.ncbi.nlm.nih.gov/entrez/query.fcgi?CMD=Pager&DB=snp>) - Search SNPs with heterozygosity between 0 and 90 percent.
- 2) SNP500Cancer (<http://snp500cancer.nci.nih.gov/snplist.cfm>) - The goal of the SNP500Cancer project is to resequence 102 reference samples to find known or newly discovered single nucleotide polymorphisms (SNPs) which are of immediate importance to molecular epidemiology studies in cancer. SNP500Cancer provides a central resource for sequence verification of SNPs.
- 3) Mreps: (<http://bioweb.pasteur.fr/seqanal/interfaces/mreps.html>) - Mreps is a flexible and efficient software program for identifying serial repeats (usually called *tandem repeats*) in DNA sequences.
- 4) GeneMarker[®] (http://www.softgenetics.com/gm/gm_fraganal.htm) for fragment analysis is a genotyping tool with an integrated pedigree function.

The eight introns of *PAX7* were scanned for genetic variations consisting of single nucleotide polymorphisms and microsatellites using the databases stated above. This practice of searching for mutations has been previously utilised elsewhere (Ceccherini, I. et al, 1994; Carrasquillo et al., 2002)

Primer & Assay Design

The primer design for microsatellite analysis was performed utilizing the Biotage AB Assay Design Software version 1.0.6. Thirty to sixty base pairs before and after the target polymorphisms were loaded into the Assay Design program to provide the best options of forward, reverse, and sequencing primers.

Location of the primers used in the investigation of the microsatellites within intron 5 and intron 8 of the *PAX7* gene.

Primer 5: rs12740463 [*Homo sapiens*] Intron 8; chromosome position: chr1:18783428+18783596

Primer	Sequence	Genotype Detail
Forward PCR Primer	CTGGGGAAGGACGAGCTGA	C: 1.000
Reverse PCR Primer	GTACCAACCGCACTGGTCATG	

Primer 16: rs2236830 [*Homo sapiens*] Intron 5; chromosome position: chr1:18726993-18727052

Primer	Sequence	Genotype Detail
Forward PCR Primer	TTTTTCCAAGGCGATCGG	T: 0.955
Reverse PCR Primer	CTGTGGCTGCCTTACCTGA	C: 0.045

P 2) rs742077 [*Homo sapiens*] Intron 8; chromosome position: chr1:18802224-18802395

Primer	Sequence	Genotype Detail
Forward PCR Primer	CCTGCAGCCTTGACCTGATTC	G: 0.080
Reverse PCR Primer	GGGAGTGTGGCTGCAATTAGAA	A: 0.920

Figure 1. Above are the primers used for the analyses of the seven samples. Given for each are: 1) the primer name, the reference SNP cluster report ID; 2) species; 3) Intron #; 4) chromosome position; 5) Genotype detail; 6) sequence of the primers.

The three sets of primers were selected based on previous research which indicated several novel cis-acting elements present in the *immediate* vicinity of SNPs detected via *In Silico* biology (Mitchell and Ziman 2006). The results of this research generated enough investigational interest to test the theories with bench work. These primers were also selected due to their positioning on the two (2) transcript variants for ARMS ([NM_013945](#) and [NM_002584](#)). The primers were also generated on the basis of the genotype detail (see above) for loss of heterozygosity. Loss of heterozygosity has been studied in ARMS previously (White *et al.* 1995; Staehelin, F. *et al.*, 2000) where chromosome 1 and chromosome 11 had exhibited chimeric translocations. In this study, we used the SNP data from previous findings (Mitchell and Ziman 2006) to test ARMS patient DNA, ERMS Cell line DNA and control genomic DNA from healthy individuals for the alleles reported in the NCBI database.

For microsatellite analysis, fluorescent dye labels (6-FAM (blue), HEX (green), and NED (yellow)) were used for each primer. Size standards (Rox (red)) are used for all samples. There is no clean-up for PCR products used in this process. One to four microliters of PCR product was used for testing. A mixture of 7.5 ul/ sample (7 ul of Hi-Di-Formamide and 0.5 uls of Rox standard) was added and then denatured at 98°C for 4 minutes and then cooled for an additional 4 minutes. Analysis of samples was performed using the 16-array 3100 Genetic Analyzer (Applied Biosystems). The analysis of the processed samples was performed with GeneMapper Software version 3.0 (Applied Biosystems) and SoftGenetics GeneMarker® version 1.51. The analysis software uses the size standard to create a standard curve for each lane and then determines the length of each dye-labeled fragment by comparing it with the standard curve for that specific lane. Accuracy of less than one base pair difference is seen between sample replicates.

***In Silico* PCR Amplification**

In-Silico PCR amplification provides the user a systematic approach to prescreen the custom-designed primers for the given template before purchase. Programs (<http://insilico.ehu.es/>) & (<http://genome.ucsc.edu/cgi-bin/hgPcr>) were used and the output of these programs allow for quick and easy changes to primer design or template choice. The two websites cited compare the user's template and primers.

PCR Analysis / Gel Electrophoresis

DNA dilution-based PCR assay was used for allele quantification and SNP detection. The following DNA concentrations (serial dilutions) were examined for the five cases; 2, 1, 0.5, 0.25, 0.125 ng/ul. One ul of each dilution was used as the DNA template for the PCR reactions. PCR was performed in a volume of 25 ul with the presence of 100 uM of each dNTP, 10 mM Tris-HCl (pH 8.3), 2 mM magnesium chloride, 50 mM potassium chloride, 0.75 unit of Taq DNA polymerase, and 15 pmoles of each custom primer. The following reaction conditions were employed: denaturation at 96°C for 5 min, followed by 60 cycles each of 1 min at 94°C, 1 min at 60°C, and 1 min at 72°C, with a final extension of 5 min at 72°C. Sixty-five cycles were used due to the small size of the fragment and the low concentration of the isolated patient DNA. Subsequently, aliquots of the PCR reaction were resolved on 2% / 4% Invitrogen™ commercial pre-cast agarose E-gel, and the products were visualized on *Bio-Rad UV Gel Doc 2000*.

Microsatellite Analysis Instrument: ABI PRISM® 3100 Genetic Analyzer

The ABI PRISM®3100 Genetic Analyzers are automated capillary electrophoresis systems that can separate, detect, and analyze fluorescent-labeled DNA fragments in one run.

RESULTS

Standard PCR Analysis/ Gel electrophoresis

Standard PCR assays performed on all seven samples revealed amplification of the selected SNPs found in the intronic regions of the *PAX7* gene (**Fig.2**). The gene-specific fragment was visualized at all dilution levels for these cases.

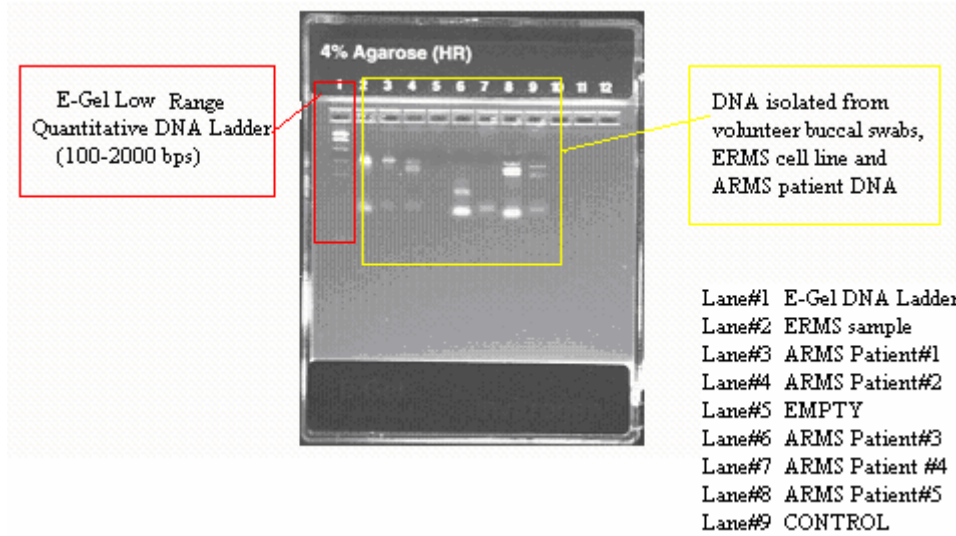


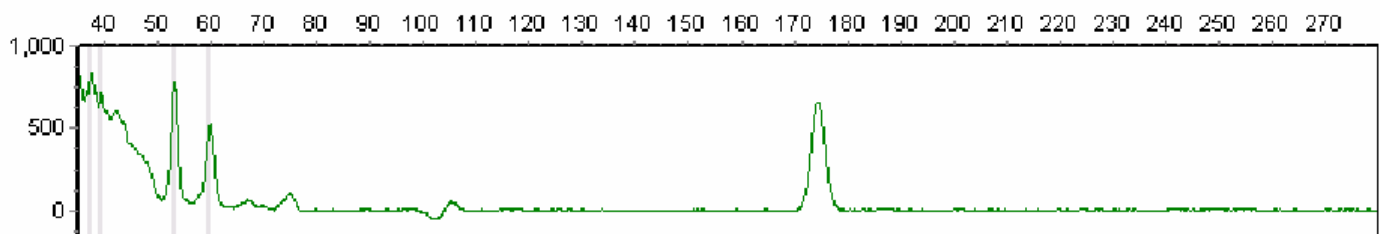
Figure 2

Figure 2. Invitrogen™ 4% precast Agarose Gel electrophoresis showing serial dilution for DNA isolated from volunteer buccal swabs, ERMS cell line and ARMS patient DNA. Sybr-Safe staining resolved on Bio-Rad UV Gel Doc 2000. All samples were exposed to the three primer sets; Primer 5 (C/T), Primer 16 (C/T), and Primer 37(G/A).

Microsatellite Analysis Results

Microsatellite Analysis provides for a visual and qualitative approach to gene copy number modifications that occur from the loss of tumor suppressor genes. In past studies, the loss of heterozygosity was detected by restriction fragment length polymorphism (RFLP) and microsatellite markers. More recently, the HuSNP GeneChip© (Affymetrix) has made the completion of large projects more attainable through allelotyping whole genomes by screening for more than 1500 SNPs in one process cycle [Wong et al., 2004].

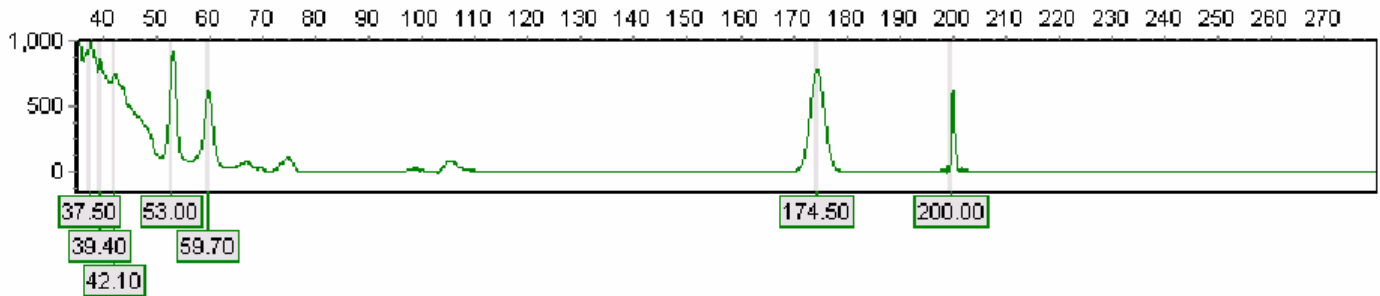
Dye: Green - 4 peaks - 1_A01_ARMS-1-5HEX_01.fsa



No	Size	Height	Area	Marker	Allele	Difference	Quality	Score	Comments
1	37.50	843	9440			1.0	Unknown	4.4	
2	39.40	710	6010			1.0	Unknown	4.6	
3	53.10	775	11531			1.0	Unknown	9.8	
4	59.80	524	8639			1.0	Unknown	3.3	

Figure 3. Fragment analysis results for ARMS Patient #1, Primer 5 with electropherogram and peak table.

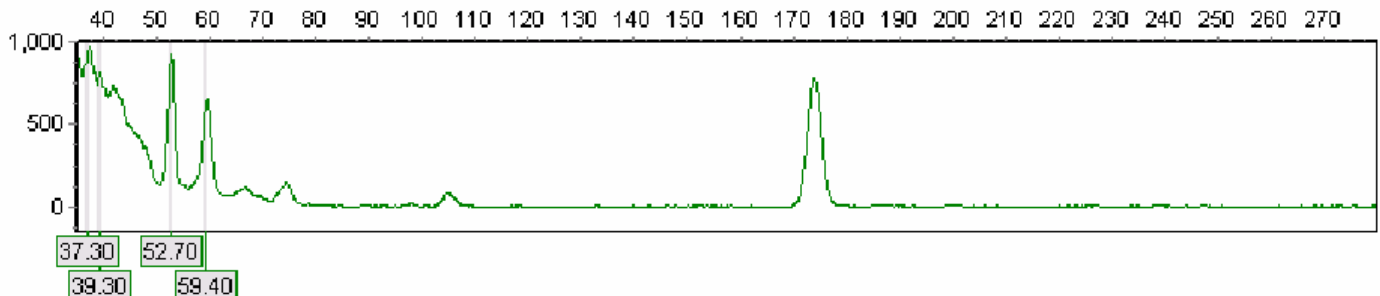
Dye: Green - 7 peaks - 1_A02_ARMS-2-5HEX_02.fsa



No	Size	Height	Area	Marker	Allele	Difference	Quality	Score	Comments
1	37.50	1015	10575			1.0	Unknown	4.4	
2	39.40	858	6540			1.0	Unknown	5.0	
3	42.10	750	9386			1.0	Unknown	1.1	
4	53.00	917	13789			1.0	Unknown	13.6	
5	59.70	625	10861			1.0	Unknown	3.9	
6	174.50	784	23081			1.0	Unknown	1.3	
7	200.00	620	3542			1.0	Unknown	78.7	

Figure 4. Fragment analysis results for ARMS Patient #2, Primer 5 with electropherogram and peak table. The presence of the mutant allele in this sample appears as an extra peak labeled with HEX (Patient#2, sample A02.205HEX) at 200 nt. The highest peak was chosen as the reference. False alleles were called when they were >5% of the most prominent allele, but were not present in the genotype of the buccal swab control DNA samples.

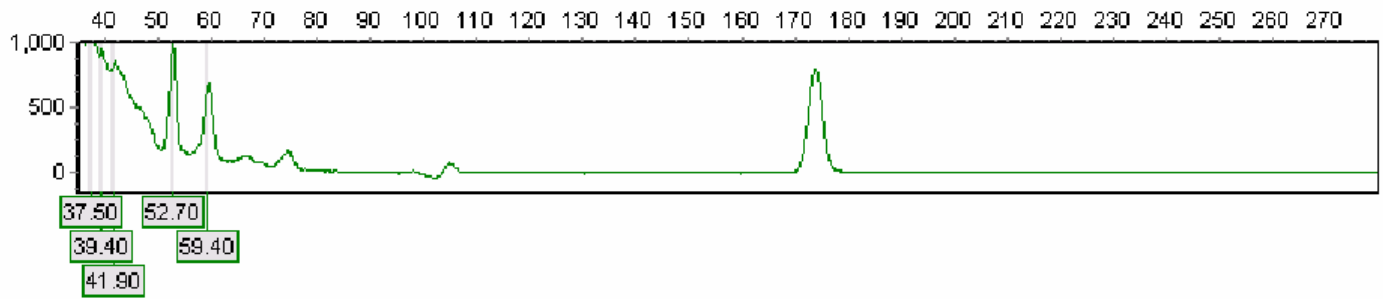
Dye: Green - 4 peaks - 1_A03_ARMS-3-5HEX_01.fsa



No	Size	Height	Area	Marker	Allele	Difference	Quality	Score	Comments
1	37.30	970	10967			1.0	Unknown	3.7	
2	39.30	819	7035			1.0	Unknown	3.6	
3	52.70	922	13713			1.0	Unknown	13.3	
4	59.40	650	11235			1.0	Unknown	4.7	

Figure 5. Fragment analysis results for ARMS Patient 31, Primer 5 with electropherogram and peak table.

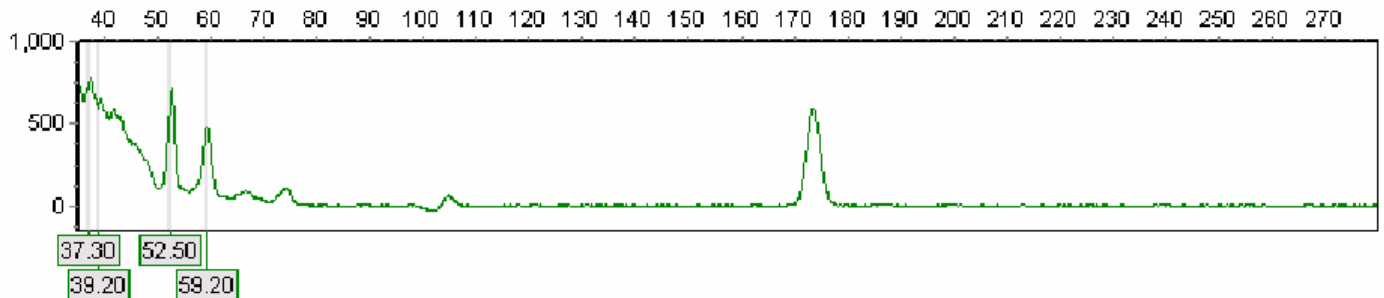
Dye: Green - 5 peaks - 1_A04_ARMS-4-5HEX_02.fsa



No	Size	Height	Area	Marker	Allele	Difference	Quality	Score	Comments
1	37.50	1145	19182			1.0	Unknown	6.0	
2	39.40	956	8254			1.0	Unknown	4.0	
3	41.90	855	10711			1.0	Unknown	1.2	
4	52.70	994	14912			1.0	Unknown	15.6	
5	59.40	684	11771			1.0	Unknown	4.6	

Figure 6. Fragment analysis results for ARMS Patient #4, Primer 5 with electropherogram and peak table.

Dye: Green - 4 peaks - 1_A05_ARMS-5-5HEX_01.fsa



No	Size	Height	Area	Marker	Allele	Difference	Quality	Score	Comments
1	37.30	772	12917			1.0	Unknown	2.1	
2	39.20	654	5604			1.0	Unknown	2.4	
3	52.50	711	10521			1.0	Unknown	9.1	
4	59.20	483	8093			1.0	Unknown	1.9	

Figure 7. Fragment analysis results for ARMS Patient #5, Primer 5 with electropherogram and peak table.

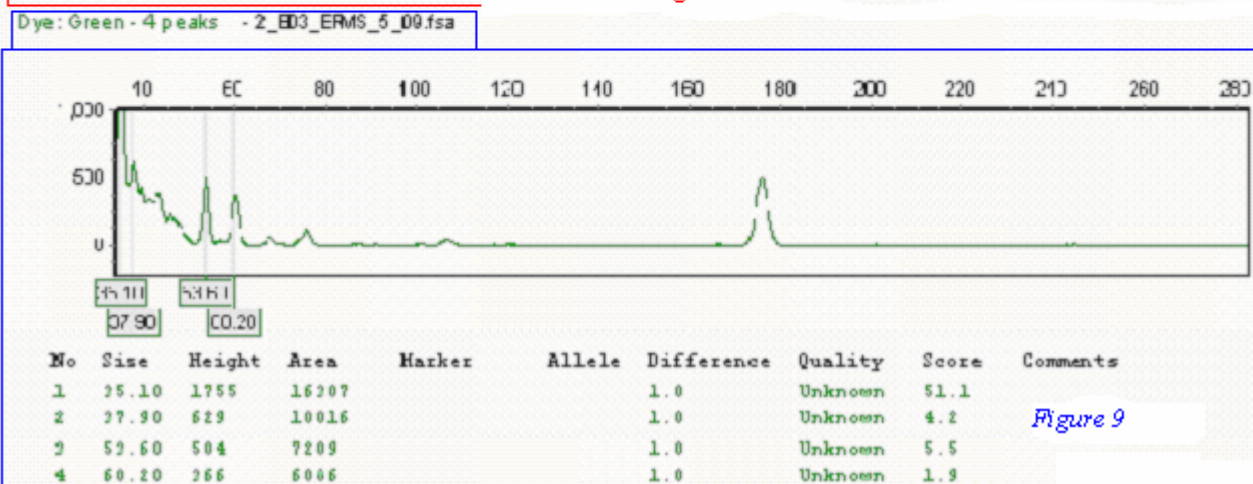
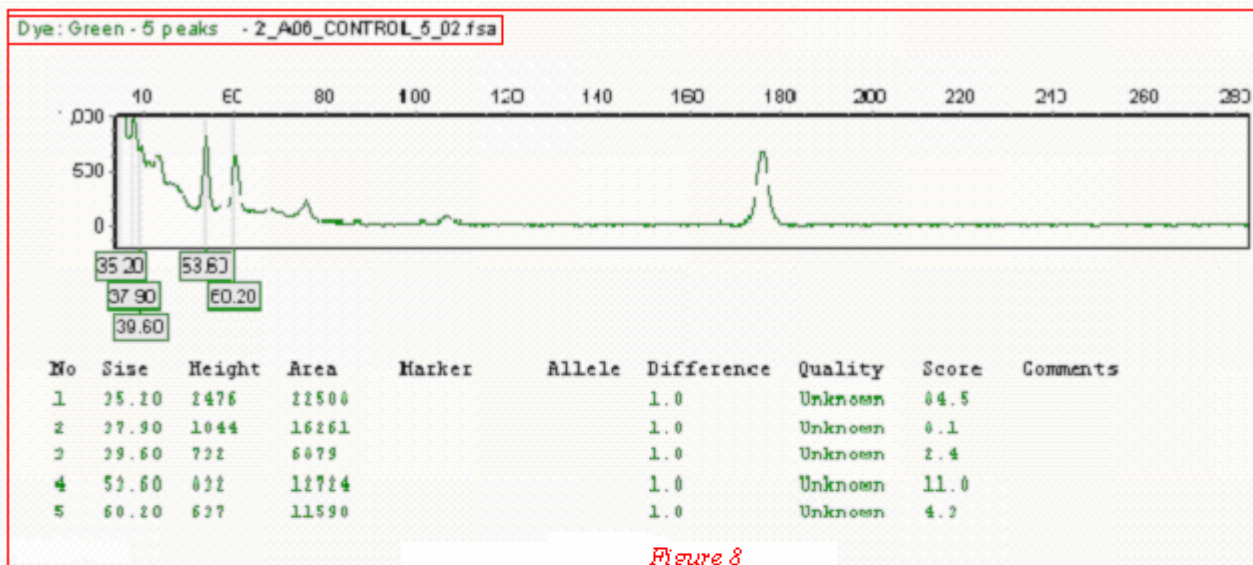


Figure 8 & Figure 9: Fragment analysis results for ERMS cell line(ATCC#: CCL 136) and control sample, with Primer 5 showing electropherograms and peak tables.

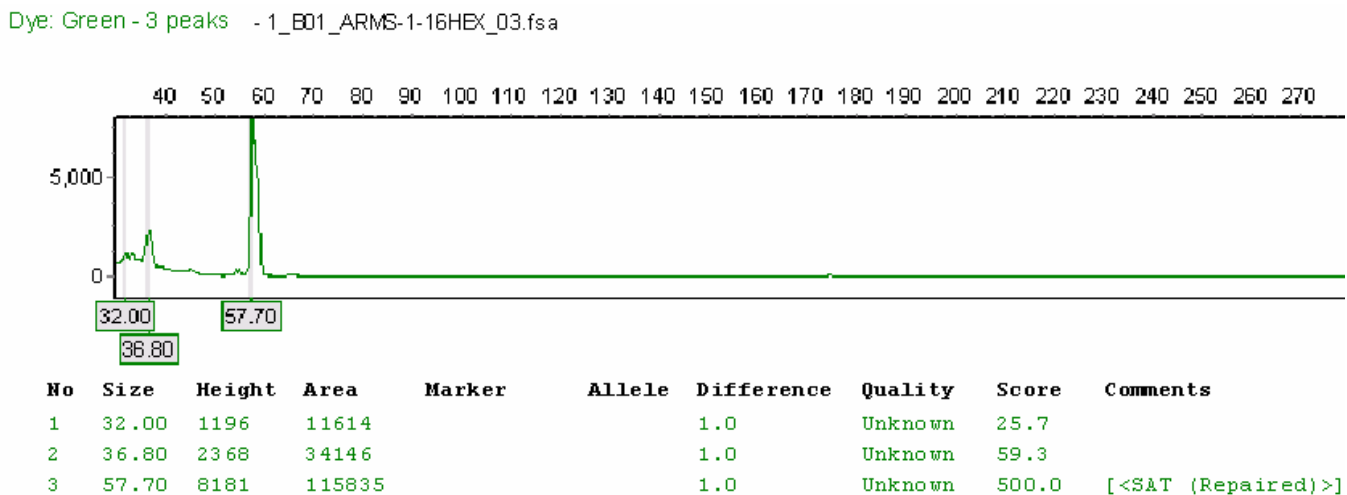


Figure 10: Fragment analysis results for ARMS Patient #1, Primer 16 with electropherogram and peak table.

Dye: Green - 5 peaks - 1_B02_ARMS-2-16HEX_04.fsa

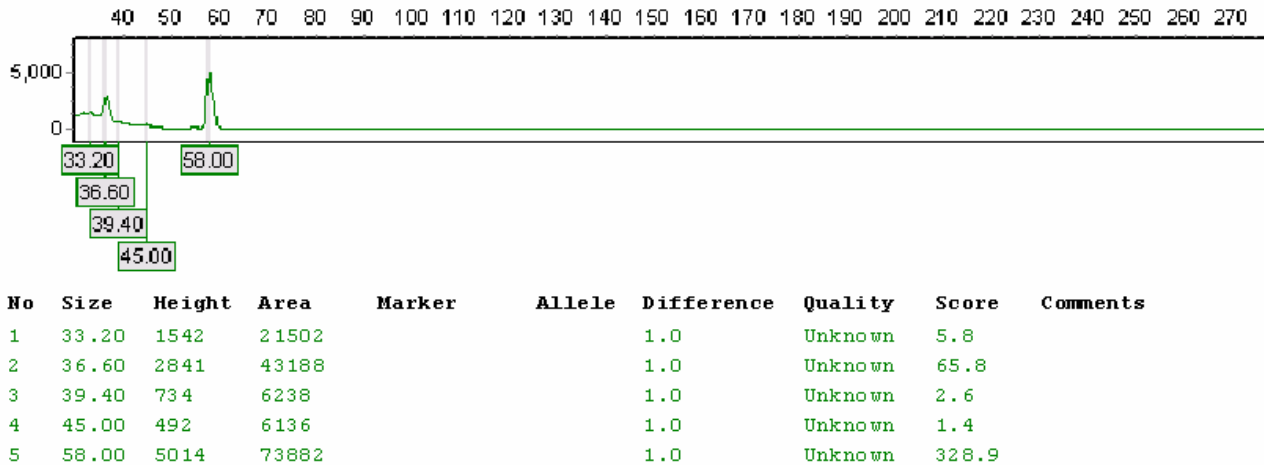


Figure 11. Fragment analysis results for ARMS Patient #2, Primer 16 with electropherogram and peak table.

Dye: Green - 4 peaks - 1_B03_ARMS-3-16HEX_03.fsa

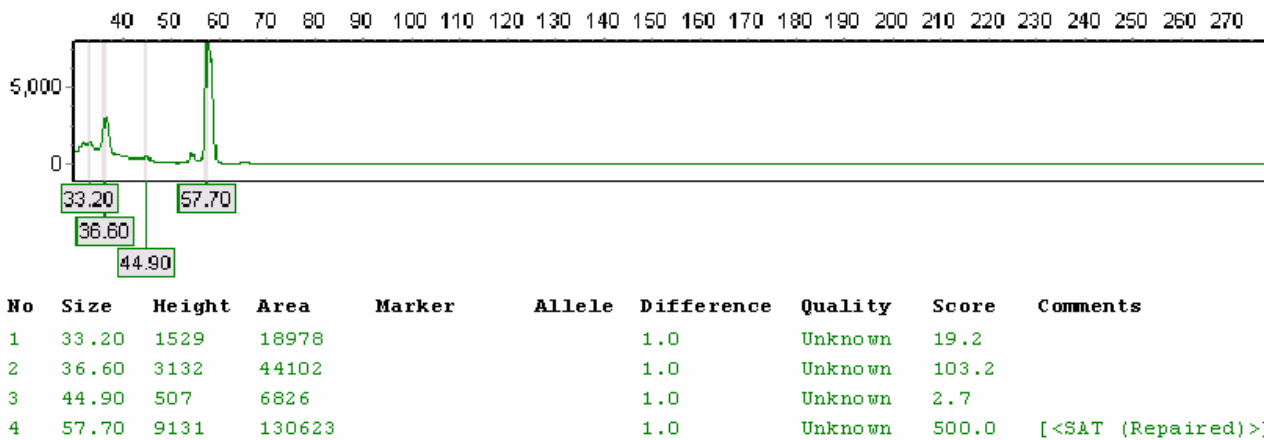


Figure 12. Fragment analysis results for ARMS Patient #3, Primer 16 with electropherogram and peak table.

Dye: Green - 4 peaks - 1_B04_ARMS-4-16HEX_04.fsa

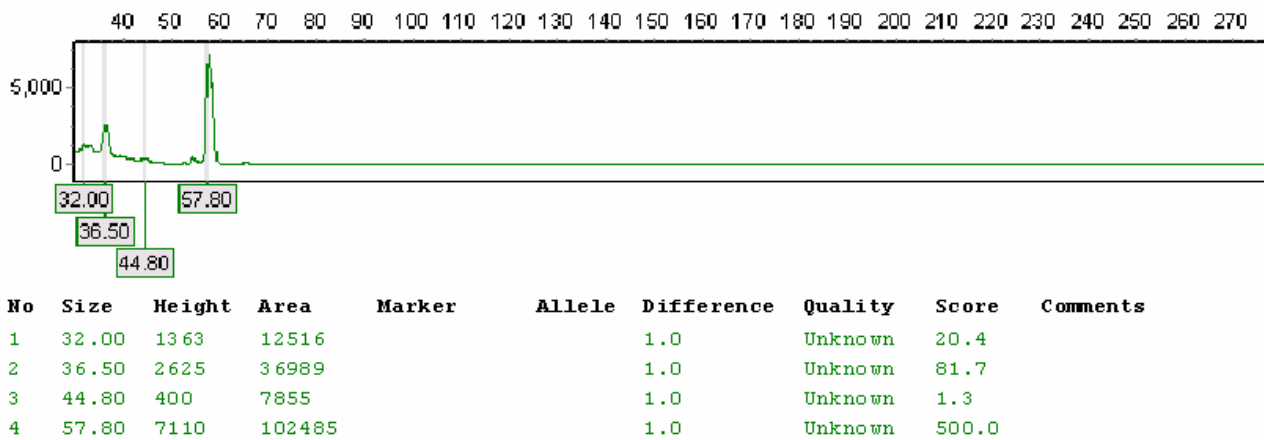
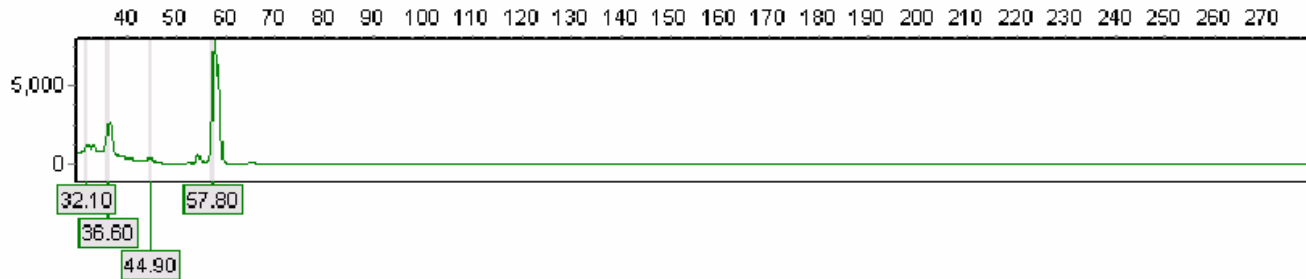


Figure 13. Fragment analysis results for ARMS Patient #4, Primer 16 with electropherogram and peak table.

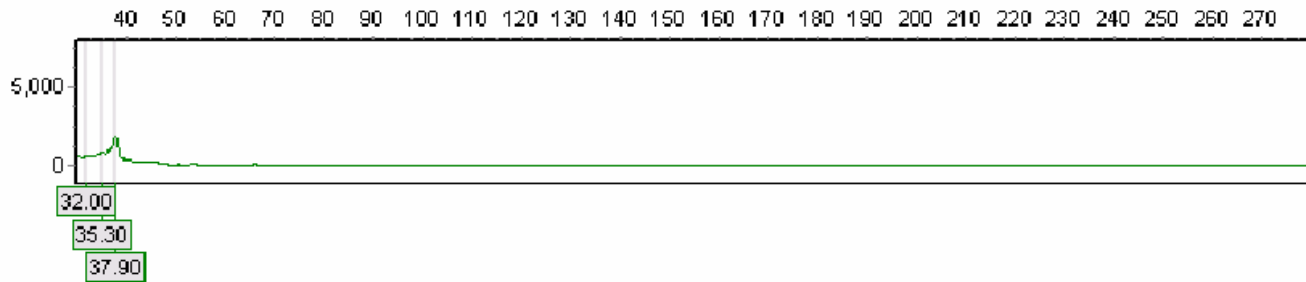
Dye: Green - 4 peaks - 1_B05_ARMS-5-16HEX_03.fsa



No	Size	Height	Area	Marker	Allele	Difference	Quality	Score	Comments
1	32.10	1297	11714			1.0	Unknown	24.6	
2	36.60	2708	36169			1.0	Unknown	94.9	
3	44.90	399	5426			1.0	Unknown	1.9	
4	57.80	7961	111354			1.0	Unknown	500.0	[<S&T (Repaired)>]

Figure 14. Fragment analysis results for ARMS Patient #5, Primer 16 with electropherogram and peak table.

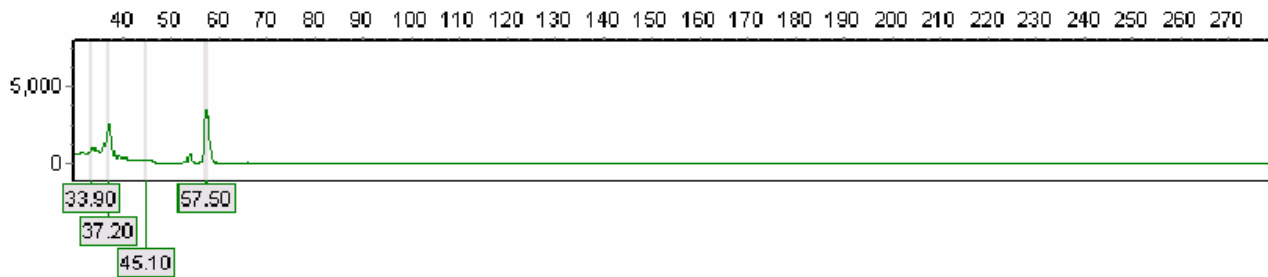
Dye: Green - 3 peaks - 2_F04_ERMS_16_12.fsa



No	Size	Height	Area	Marker	Allele	Difference	Quality	Score	Comments
1	32.00	701	7803			1.0	Unknown	3.0	
2	35.30	905	16647			1.0	Unknown	3.8	
3	37.90	1921	23720			1.0	Unknown	61.5	

Figure 15. Fragment analysis results for ERMS Cell line (ATCC#: CCL 136), Primer 16 with electropherogram and peak table. Note: Peak 57.50 is absent from this sample.

Dye: Green - 4 peaks - 2_D01_16_control_2ul_07.fsa



No	Size	Height	Area	Marker	Allele	Difference	Quality	Score	Comments
1	33.90	991	19417			1.0	Unknown	3.7	
2	37.20	2584	35117			1.0	Unknown	107.5	
3	45.10	331	5111			1.0	Unknown	1.4	
4	57.50	3474	30708			1.0	Unknown	392.3	

Figure 16. Fragment analysis results for CONTROL sample (genomic DNA) with Primer 16 with electropherogram and peak table.

Dye: Green - 4 peaks - 2_D01_ARMS_1_37_07.fsa

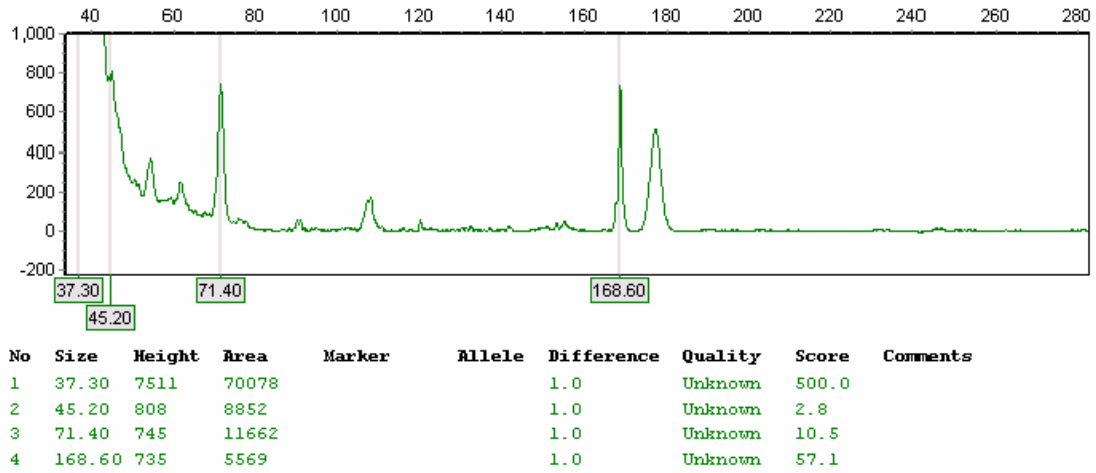


Figure 17. Fragment analysis results for ARMS Patient #1, Primer 37 with electropherogram and peak table.

Dye: Green - 9 peaks - 2_D02_ARMS_2_37_08.fsa

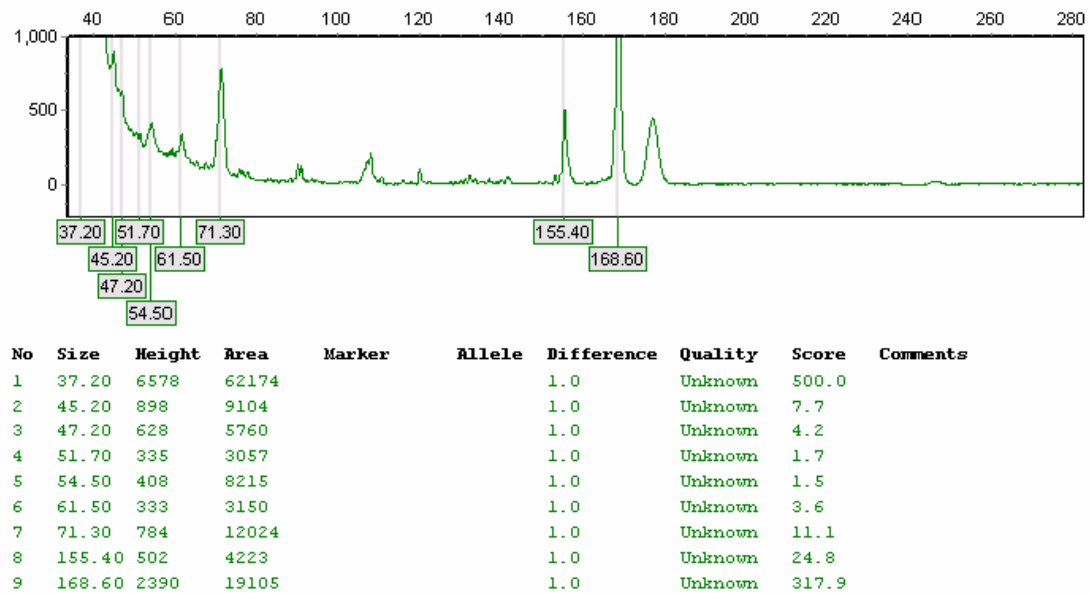


Figure 18. Fragment analysis results for ARMS Patient #2, Primer 37 with electropherogram and peak table.

Dye: Green - 3 peaks - 2_D03_ARMS_3_37_07.fsa

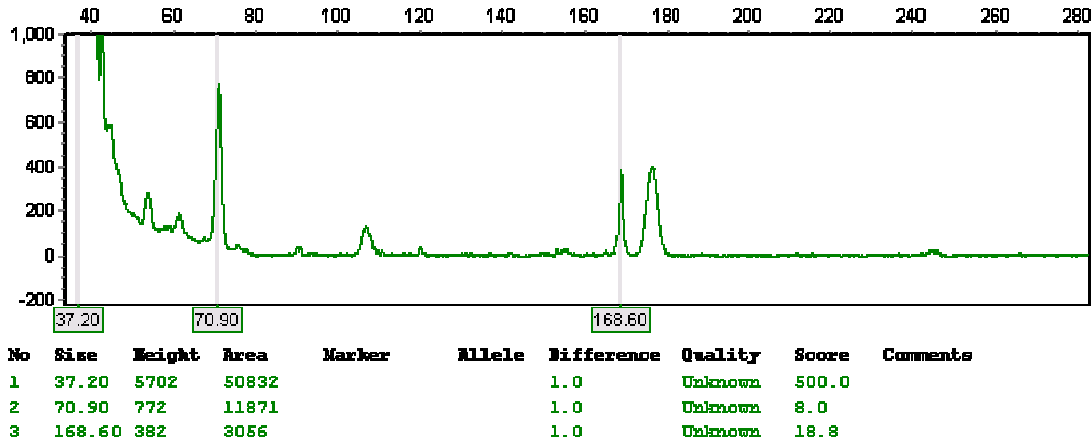


Figure 19. Fragment analysis results for ARMS Patient #3, Primer 37 with electropherogram and peak table.

Dye: Green - 3 peaks - 2_D04_ARMS_4_37_08.fsa

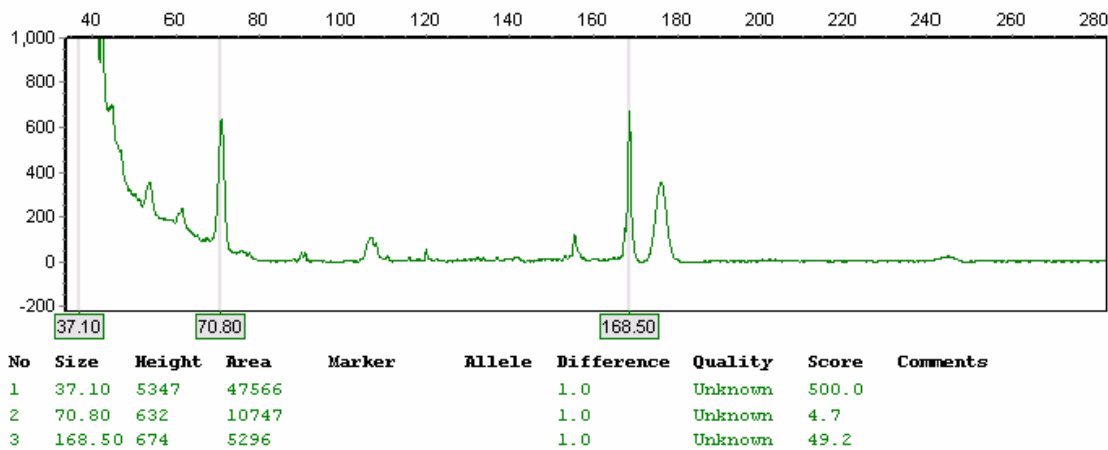


Figure 20. Fragment analysis results for ARMS Patient #4, Primer 37 with electropherogram and peak table.

Dye: Green - 5 peaks - 2_D05_ARMS_5_37_07.fsa

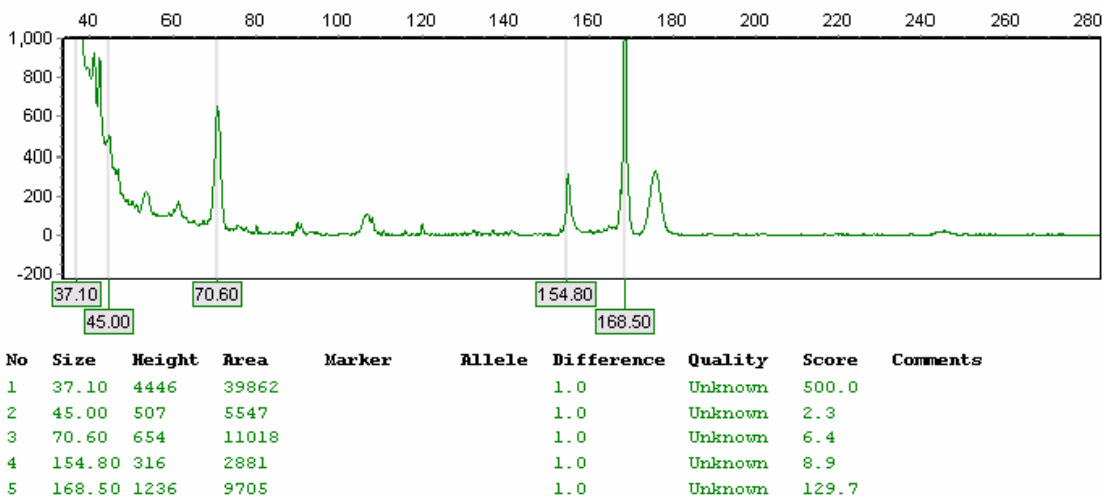
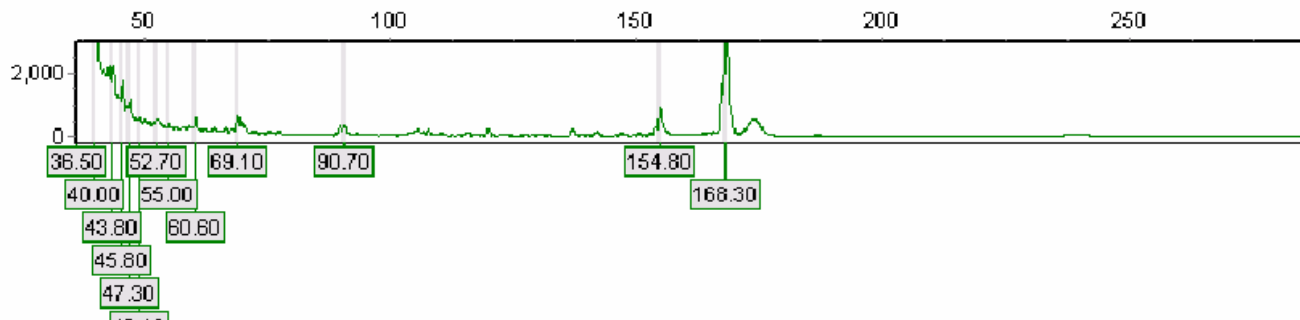


Figure 21. Fragment analysis results for ARMS Patient #5, Primer 37 with electropherogram and peak table.

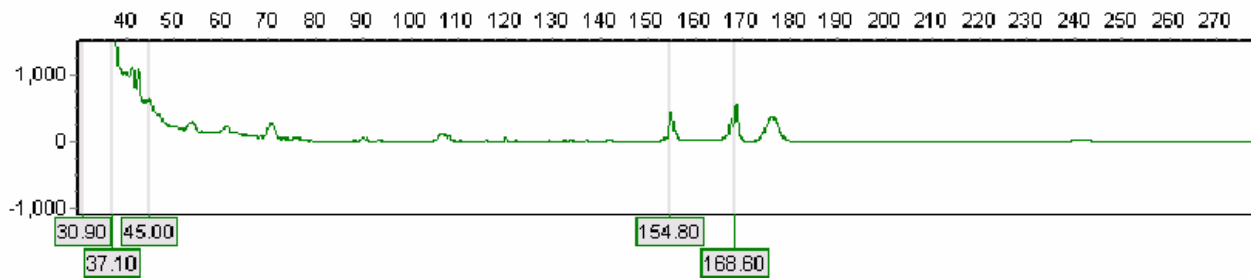
Dye: Green - 14 peaks - 2_B01_37_control_2ul_03.fsa



No	Size	Height	Area	Marker	Allele	Difference	Quality	Score	Comments
1	35.00	7052	45223			1.0	Unknown	408.9	
2	36.50	7546	117513			1.0	Unknown	302.1	
3	40.00	8766	63976			1.0	Unknown	500.0	[<SAT (Repaired)>]
4	43.80	2258	17471			1.0	Unknown	104.6	
5	45.80	1740	12469			1.0	Unknown	157.0	
6	47.30	1166	8479			1.0	Unknown	59.7	
7	49.10	602	4295			1.0	Unknown	10.0	
8	52.70	558	10166			1.0	Unknown	2.0	
9	55.00	394	2791			1.0	Unknown	6.1	
10	60.60	575	4245			1.0	Unknown	36.3	
11	69.10	679	4353			1.0	Unknown	64.0	
12	90.70	382	2343			1.0	Unknown	28.8	
13	154.80	884	6906			1.0	Unknown	68.4	
14	168.30	4817	35291			1.0	Unknown	500.0	

Figure 22. Fragment analysis results for CONTROL sample (genomic DNA) with Primer 37 with electropherogram and peak table.

Dye: Green - 5 peaks - 2_G03_ERMS_37_13.fsa



No	Size	Height	Area	Marker	Allele	Difference	Quality	Score	Comments
1	30.90	7034	73699			1.0	Unknown	386.2	
2	37.10	5093	44949			1.0	Unknown	500.0	
3	45.00	630	10027			1.0	Unknown	2.0	
4	154.80	446	3950			1.0	Unknown	20.6	
5	168.60	555	4205			1.0	Unknown	36.5	

Figure 23. Fragment analysis results for ERMS Cell line (ATCC#: CCL 136), Primer37 with electropherogram and peak table.

DISCUSSION

The microsatellite results for all sample types were normal or within the percentage range based on the genotypes detailed on the National Center for Biotechnology Information website (<http://www.ncbi.nlm.nih.gov/>). However, significant results from this study indicate that ARMS patient#2 (Figure#4) when analysed by microsatellite analysis exhibited a definite mutation for primer 5 as compared to the other 4 ARMS patients, the ERMS cell line sample and the control. Patient #2 sample may possess microsatellite instability, (MSI) which is noted for many other types of tumors [Van Dyke et al., 1994]. The presence of the additional microsatellite (Figure#4) is associated with genomic instability, giving rise to mutations that involve the addition or subtraction of one or two repeat units. This may or may not be dependent on the site of this locus on the *PAX7* gene.

There was a deletion observed in the ERMS cell line by analysis with Primer 16 (Figure#15), which is located at the 3' of intron 5. This may be an aberration cause by the immortalization process of the RD cells. The particular cell line used, ATCC – CCL-136™, is isolated from muscle tissue of a female *Homo sapiens* fetus and consists of spindle cells and large multinucleated cells. The medium in which these adherent cells are stored is Dulbecco's modified Eagle's medium with 4 mM L-glutamine adjusted to contain 1.5 g/L sodium bicarbonate and 4.5 g/L glucose, 90%; fetal bovine serum, 10% and DMSO, 5% at a temperature of 37° Celsius. DMSO can inhibit certain types of reactions (i.e. Big Dye Terminator reactions used in DNA sequencing) which may explain why the peak which is present in the other sample types including the control, is absent in the ERMS sample.

Recessive oncogenic alterations typically lead to the biallelic inactivation of tumor suppressor genes [Cavenee et al., 1983]. Alterations such as homozygous and heterozygous deletions or gene conversions are thought to be among the most common genetic abnormalities in epithelial cancers and their detection using LOH analysis is becoming common and essential to the discovery of genes targeted by such events [Lindblad-Toh et al., 2000]. Oligonucleotide microarrays, capable of simultaneously determining the genotype of 1494 SNPs, have been used to map regions of LOH in small cell lung, breast, bladder, and prostate cancer [Primdahl et al., 2002; Schubert et al., 2002; Dumur et al., 2003; Hoque et al., 2003; Lieberfarb et al., 2003]. In small cell lung cancer, detection of regions of LOH using SNP arrays was shown to be comparable with LOH detection using microsatellite markers but required cancer cell purity of $\geq 90\%$ [Schubert et al., 2002].

Regions of LOH, usually arising as a result of either hemizygous deletion or gene conversion events, are typically defined as stretches of chromosomal areas where all heterozygous and thereby informative alleles are rendered homozygous in the cancer. The boundaries of such regions of LOH are defined by either the presence of retained heterozygous alleles, the ends of chromosomal arms, or the centromere. This classical definition assumes that all data points are completely accurate and that all polymorphic alleles are mapped correctly within the genome [Van Dyke et al., 1994; Davis et al., 1997].

Although previous research has shown where mutations within introns can affect phenotypes [White et al., 1995; Howe et al., 1997; Girard et al., 2000; Sun et al., 2000; Mattick et al., 2001; O'Keefe, 2002; Howe et al., 2003; Goodarzi et al., 2005; Beauchemin et al., 2006] the novelty of these finding is merely a start. At this point in time the significance of finding a mutation in one patient and a deletion in one ERMS cell line is not known but may prove to be vital for future testing of these sarcomas and may ultimately enable improved diagnosis and outcomes in patients with Alveolar Rhabdomyosarcoma and Embryonal Rhabdomyosarcoma.

Acknowledgments

We would also like to thank the Memorial Sloan Kettering Institute DNA Sequencing Core Facility and Memorial Sloan Kettering Cancer Center's Diagnostic Molecular Laboratory for their support and assistance for the clinical portions of this project.

REFERENCES

Kelloff, Gary J., Lippman, Scott M., et al, for the AACR Task Force on Cancer Prevention, Progress in Chemoprevention Drug Development: The Promise of Molecular Biomarkers for Prevention of Intraepithelial Neoplasia and Cancer--A Plan to Move Forward Clin Cancer Res 2006 12: 3661-3697

Maris, John M., Hii, George, Gelfand, Craig A., Varde, Shobha, White, Peter S., Rappaport, Eric, Surrey, Saul, Fortina, Paolo Region-specific detection of neuroblastoma loss of heterozygosity at multiple loci simultaneously using a SNP-based tag-array platform Genome Res. 2005 15: 1168-1176

Hirsch, Fred R., Franklin, Wilbur A., Gazdar, Adi F., Bunn, Paul A., Jr. Early Detection of Lung Cancer: Clinical Perspectives of Recent Advances in Biology and Radiology Clin Cancer Res 2001 7: 5-22

Loh WE, HJ Scrabble, E Livanos, MJ Arboleda, WK Cavenee, M Oshimura & BE Weissman: Human chromosome 11 contains two different growth suppressor genes for embryonal rhabdomyosarcoma. Proc Natl Acad Sci USA 1992 89, 1755-1759

Wong, Kwok, Tsang Y. et al., Allelic imbalance analysis by high density single nucleotide polymorphic allele (SNP) array with whole genome amplified DNA. Nucl Acids Research, 2004, 32, 1-8.

Kathleen M. Murphy, Karin D. Berg, and James R. Eshleman, Sequencing of Genomic DNA by Combined Amplification and Cycle Sequencing Reaction, Clin Chem 2005, 51, 35-39.

Sanger F, Nicklen S, Coulson AR. DNA sequencing with chain-terminating inhibitors. Proc Natl Acad Sci U S A 1977, 74:5463-5467.

Nyr'en, Pettersson & Uhl'en 'Solid phase DNA minisequencing by an enzymatic luminometric inorganic pyrophosphate detection assay', Anal. Biochem. 1993, 208, 171-175.

Knudson A. G., Jr. Mutation and cancer: statistical study of retinoblastoma. Proc. Natl. Acad. Sci. USA, 68: 820-823, 1971

Cavenee W. K., Dryja T. P., Phillips R. A., Benedict W. F., Godbout R., Gallie B. L., Murphree A. L., Strong L. C., White R. L. Expression of recessive alleles by chromosomal mechanisms in retinoblastoma. Nature (Lond.), 305: 779-784, 1983.

Lindblad-Toh K., Tanenbaum D. M., Daly M. J., Winchester E., Lui W. O., Villapakkam A., Stanton S. E., Larsson C., Hudson T. J., Johnson B. E., Lander E. S., Meyerson M. Loss-of-heterozygosity analysis of small-cell lung carcinomas using single-nucleotide polymorphism arrays. Nat. Biotechnol., 18: 1001-1005, 2000

Schubert E. L., Hsu L., Cousens L. A., Glogovac J., Self S., Reid B. J., Rabinovitch P. S., Porter P. L. Single nucleotide polymorphism array analysis of flow-sorted epithelial cells from frozen versus fixed tissues for whole genome analysis of allelic loss in breast cancer. Am. J. Pathol., 160: 73-79, 2002.

Dumur C. I., Dechsukhum C., Ware J. L., Cofield S. S., Best A. M., Wilkinson D. S., Garrett C. T., Ferreira-Gonzalez A. Genome-wide detection of LOH in prostate cancer using human SNP microarray technology. Genomics, 81: 260-269, 2003.

Hoque M. O., Lee C. C., Cairns P., Schoenberg M., Sidransky D. Genome-wide genetic characterization of bladder cancer: a comparison of high-density single-nucleotide polymorphism arrays and PCR-based microsatellite analysis. Cancer Res., 63: 2216-2222, 2003.

Primdahl H., Wikman F. P., von der Maase H., Zhou X. G., Wolf H., Orntoft T. F. Allelic imbalances in human bladder cancer: genome-wide detection with high-density single-nucleotide polymorphism arrays. J. Natl. Cancer Inst. (Bethesda), 94: 216-223, 2002.

Lieberfarb, Marshall E., Lin, Ming, Lechpammer, Mirna, Li, Cheng, Tanenbaum, David M., Febbo, Phillip G., Wright, Renee L., Shim, Judy, Kantoff, Philip W., Loda, Massimo, Meyerson, Matthew, Sellers, William R. Genome-wide Loss of Heterozygosity Analysis from Laser Capture Microdissected Prostate Cancer Using Single Nucleotide Polymorphic Allele (SNP) Arrays and a Novel Bioinformatics Platform dChipSNP Cancer Res 2003 63: 4781-4785.

Van Dyke, D.L.; Worsham, M.J.; Zarbo, R.J. Loss of heterozygosity and microsatellite instability in chromosomal segments commonly deleted in squamous cell carcinoma. American Journal of Human Genetics; 1994. VOL. 55; ISSUE: Suppl.3; 44.

Mitchell, Maika G., Ziman, Melanie. An In Silico Investigation into the Discovery of Novel Cis-acting Elements within the Intronic Regions of Human PAX7. *Nature & Science*. **2006**. Volume 4 (3)12:69-85.

Davis, R.J. and Barr, F.G., Fusion genes resulting from alternative chromosomal translocations are overexpressed by gene-specific mechanisms in alveolar rhabdomyosarcoma. *Proc Natl Acad Sci U S A*. **1997** July 22; 94(15): 8047–8051.

Steenman MJC, Zijlstra N, Kruitbosch DL, Wiesmeijer C, Larizza L, Voûte PA, Westerveld A, Mannens MMAM:Delineation and physical separation of novel translocation breakpoints on chromosome 1p in two genetically closely associated childhood tumors. *Cytogenet Cell Genet* **2000**;88:289-295.

Gattenlöhner, Stefan; Müller-Hermelink, Hans-Konrad; Marx, Alexander., Polymerase Chain Reaction-Based Diagnosis of Rhabdomyosarcomas: Comparison of Fetal Type Acetylcholine Receptor Subunits and Myogenin. *Diagnostic Molecular Pathology: Volume 7(3) June 1998* pp 129-134.

Dolan, Eileen, M. Carboxylesterase Project. Project focuses on identifying single nucleotide polymorphisms (SNPs) in human carboxylesterase I and/or II responsible for phenotypic variability in CPT-11 conversion to SN-38. **2002**.

Beauchemin et al., Evaluation of DNA polymorphisms involving growth hormone relative to growth and carcass characteristics in Brahman steers. *Genet. Mol. Res.* 5 (3): 438-447 **2006**.

Girard, Lisa, Freeling, Michael Mutator-Suppressible Alleles of rough sheath1 and liguleless3 in *Genetics* **2000** 154: 437-446.

Raymond T. O'Keefe. Mutations in U5 snRNA loop 1 influence the splicing of different genes in vivo *Nucl. Acids Res.* **2002** 30: 5476-5484.

Howe, J.K. Ares, M., Intron self-complementarity enforces exon inclusion in a yeast pre-mRNA. *Proc. Natl. Acad. Sci. USA* Vol. 94, pp. 12467–12472, **1997**.

Mark O. Goodarzi, Howard Wong, Manuel J. Quiñones, Kent D. Taylor, Xiuqing Guo, Lawrence W. Castellani, Heath J. Antoine, Huiying Yang, Willa A. Hsueh, and Jerome I. Rotter. The 3' Untranslated Region of the Lipoprotein Lipase Gene: Haplotype Structure and Association with Post-Heparin Plasma Lipase Activity *J. Clin. Endocrinol. Metab.* 90: 4816-4823. **2005**.

Sun et al., Nonsense-mediated decay of glutathione peroxidase 1 mRNA in the cytoplasm depends on intron position. *EMBO J.* **2000** September 1; 19(17): 4734–4744.

John S. Mattick and Michael J. Gagen .The Evolution of Controlled Multitasked Gene Networks: The Role of Introns and Other Noncoding RNAs in the Development of Complex Organisms. **2001**.*Mol Biol Evol* 18: 1611-1630.

Howe et al., Perturbation of transcription elongation influences the fidelity of internal exon inclusion in *Saccharomyces cerevisiae* RNA. **2003**. 9:993–1006.

PS White, JM Maris, C Beltinger, E Sulman, HN Marshall, M Fujimori, BA Kaufman, JA Biegel, C Allen, C Hilliard, MB Valentine, AT Look, H Enomoto, S Sakiyama, and GM Brodeur A Region of Consistent Deletion in Neuroblastoma Maps within Human Chromosome 1p36.2-36.3. **1995**. *PNAS* 92: 5520-5524.

Stahelin, F. et al., Inv(11)(p13p15) and Myf-3(MyoD1) in a Malignant Extrarenal Rhabdoid Tumor of a Premature Newborn. *Pediatr Res* 48:**2000**. 463-467.

Carrasquillo, Minerva M., McCallion, Andrew S., Puffenberger, Erik G., Kashuk, Carl S., Nouri, Nassim., Chakravarti, Aravinda Genome-wide association study and mouse model identify interaction between RET and EDNRB pathways in Hirschsprung disease. *Nat Genet* . **2002**.

Ceccherini, I. et al. Identification of the Cys634Tyr mutation of the RET proto-oncogene in a pedigree with multiple endocrine neoplasia type 2A and localized cutaneous lichen amyloidosis. *J. Endocrinol. Invest.* 17, 201–204 (1994).